SOLUTION MINING RESEARCH INSTITUTE
105 Apple Valley Circle
Clarks Summit, PA 18411, USA

Telephone: +1 570-585-8092
Fax: +1 505-585-8091
www.solutionmining.org

Technical Conference Paper

Set-up of a broken-casings detection system

Benoit Brouard
Brouard Consulting, Paris, France

Pierre Bérest, Vincent de Greef, Gérard Gary
Ecole Polytechnique, Palaiseau, France

Pierre Gillard, Marc Valette
Arkema, Vauvert, France

SMRI Spring 2012 Technical Conference
23 – 24 April 2012
Regina, Saskatchewan, Canada

Solution Mining Research Institute Spring 2012 Technical Conference

Regina, Saskatchewan, Canada, 23 – 24 April 2012

SET-UP OF A BROKEN-CASINGS DETECTION SYSTEM

Benoît Brouard, Brouard Consulting, Paris, France

Pierre Bérest, Vincent de Greef, Gérard Gary, Ecole Polytechnique, France

Pierre Gillard, Marc Valette, Arkema, Vauvert, France

Abstract

Water hammers commonly are observed at wellheads and often are considered a potential hazard that should be avoided. Nevertheless, there are a few situations in which water hammers provide very valuable information about a well. A comprehensive data-acquisition and analysis system has been developed by Brouard Consulting and Ecole Polytechnique. One potential application of that system is determining the depth of the final string; this application has been tested successfully at Vauvert brine field. It is demonstrated here that this low-cost and non-intrusive system is accurate and allows practical, real-time measurements.

Key words: Instrumentation and Monitoring, Computer Modeling/Software, Well Casing, Well Logging

1. Introduction

In the solution-mining industry, there are several situations in which it is useful — or even necessary — to know precisely the final length of a hanging string or the depth of an interface between two fluids. Two examples are given below.

> ***Example 1: Hanging tubulars*** — Damaged string is a well–known issue:
>
> *Brine strings are essential components of both natural gas and liquid hydrocarbon storage caverns. (…) If the brine injection or brine withdrawal velocity is gradually increased, eventually, the hanging tubular will experience flow–induced vibration, resulting in the potential for the hanging tubulars to bend and/or break. Additionally, in both types of hydrocarbon storage, salt falls can impact the brine string integrity.* (Ratigan, 2008).
>
> ***Example 2: MITs*** — When performing an MIT (Van Sambeek et al., 2005), it is usually necessary to measure the displacement of an interface between nitrogen and brine (Nitrogen Leak Test) or between two liquids (Liquid–Liquid Test).

In the first example, a damaged (or even broken) string often is not detected in real time. In the second example, an interface-level measurement usually is taken only at the beginning and end of an MIT. In both cases, a relatively costly logging operation is required to obtain the needed data.

Subsequently, it is appealing to build a non-invasive system that would permit accurate determination of the final lengths of strings or of interface depths, especially **in real time** and **at low cost**.

2. Usefulness of water hammers

2.1 Introduction

When the momentum of the fluid in a wellbore or other piping system is changed rapidly, flow is initiated locally, and a pressure wave is transmitted through the fluid. The pressure wave produced at shut–in travels the length of the well, is reflected at the bottom and returns to the surface, where it is reflected again. The wave travels in the fluid at the speed of sound. This process continues until the wave is completely damped by frictional processes within the fluid and along the casing walls.

For many years, Brouard Consulting and Ecole Polytechnique have measured, and studied water hammers and, more generally, oscillatory phenomena in storage wells and salt caverns (Bérest et al., 1996 and 1999). Because water hammers are easy to measure and, because the related pressure evolution depends on well properties, there are many circumstances when it can be useful to analyze water hammers to back-calculate some parameters —for instance, the final length of the well or the depth of the interface between two fluids.

2.2 Wave celerity

If the casing were perfectly stiff, the acoustic wave celerity c_f (m/s) would be given by the simple formula

$$c_f = 1/\sqrt{\rho_f \beta_f^{ad}} \tag{1}$$

where ρ_f is fluid density (kg/m3), and β_f^{ad} is its adiabatic coefficient of compressibility (/Pa). Typical celerities are $c_w = 1500$ m/s (4500 ft/s) for soft water and $c_b = 1800$ m/s (5600 ft/s) for saturated brine.

In fact, a steel casing surrounded by cement and rock is also a compressible body. Its compressibility factor, β_c, can be calculated theoretically if the characteristics of the casing and its environment are perfectly known — which will hardly be the case. In any case, the global well-compressibility factor, $\beta = \beta_f^{ad} + \beta_c$, is larger than β_f^{ad}, resulting in a speed of sound, c, in the well that is smaller than the speed of the fluid wave:

$$1/c^2 = 1/c_f^2 + \rho_f \beta_c \tag{2}$$

2.3 Water–hammer amplitude

Joukowsky's fundamental equation of water (1898) allows calculation of water–hammer amplitude, ΔP, as a function of velocity change, Δv, fluid density and acoustic wave speed:

$$\Delta P = \rho_f c \Delta v \tag{3}$$

2.4 Wave propagation

Euler's differential equation for momentum is written

$$\rho_0 \frac{\partial v(z,t)}{\partial t} + \frac{\partial P'(z,t)}{\partial z} + \frac{4}{d}\tau_w = 0 \tag{4}$$

where v is the fluid velocity, which is a function of depth (z) and time (t), P' is the pressure variation, d is the inner diameter of the casing, and τ_w is the shear stress at the casing wall.

Several models can be found in the literature for calculating the shear stress; a comprehensive list is given by Ghidaoui et al. (2005).

2.4 Boundary conditions

When the wave reaches a change in well cross-section, S, or an interface with another fluid, part of the wave is reflected back to the ground, while a complementary part is transmitted downward. Generally speaking, the energy reflection ratio, R, and transmission ratio, T, are functions of acoustic impedance, Z, variations:

$$R = \left(\frac{Z_2 - Z_1}{Z_1 + Z_2} \right)^2 \qquad T = \frac{4 Z_1 Z_2}{\left(Z_1 + Z_2 \right)^2} \qquad \text{where} \qquad Z_i = \frac{\rho_f^i c_i}{S_i} \tag{5}$$

These ratios hold for the intensities of energy flux in the waves — i.e., they are related to energy conservation ($R + T = 1$). With regard to pressure and velocity amplitudes, there is no conservation rule, and reflection and transmission coefficients are as follows:

$$r_p = \frac{Z_2 - Z_1}{Z_1 + Z_2} \qquad t_p = \frac{2 Z_2}{Z_1 + Z_2} \qquad \text{and} \qquad r_v = \frac{Z_1 - Z_2}{Z_1 + Z_2} \qquad t_v = \frac{2 Z_1}{Z_1 + Z_2} \tag{6}$$

Where $\left(r_p, t_p \right)$ are coefficients for pressure and $\left(r_v, t_v \right)$ for velocity.

When the wave reaches the cavern

When the wave reaches the end of the last string in a large cavern, it is reflected almost completely, as the wave is not able to modify the pressure in the cavity by any noticeable amount. Then, a second wave, travelling upward and transporting an opposite pressure of same magnitude, is generated such that the pressure change that had been generated by the primary downward wave vanishes to zero below the upward wave. This wave reaches the wellhead, being reflected and is transmitted at any cross-section change or fluid change —in turn, generating a downward wave. After a short time, these waves combine to form a simple stationary wave; pressure changes, P', or fluid velocity, v, have the same phase along the entire well. These stationary waves are dampened; the highest frequency components rapidly vanish, leaving a simpler wave whose periods are fixed by the boundary conditions.

An example of stationary wave envelopes is given in Figure 9 for the case of the PA31 well, which is composed of three different cross-sections (Figure 3). Envelopes of pressure variations (left) and velocity (right) for the two first modes (fundamental and second harmonic) are plotted. When the wellhead is shut in, it becomes a pressure node and a velocity antinode. (Velocity is null at the wellhead.) Alternatively, the casing shoe in the cavern is a velocity node and a pressure antinode. For this example, a 1-bar pressure amplitude at the wellhead relates to a 6.3 cm/s (2.5 in/s) fluid velocity at the casing shoe.

3. Application to the measurement of the casing length at Vauvert

3.1 Vauvert facility

Arkema produces brine at its Vauvert facility in southern France by solution mining at a depth ranging from 1900 m (6000 ft) to 3000 m (10,000 ft). The salt has been leached out between pairs or triples of wells since the 1970s. Connection between wells is obtained by hydrofracturing.

The local geology is very complex (Figure 1) and was the subject of a Ph.D. thesis by Valette (1991). There is an abnormal superposition of a saliferous syn–rift series of Stampian age (Oligocene) in the northeastern part of the Camargue basin extension. This abnormal superposition results from North–

Westward thrusting along two ramps that splay from an intra–saliferous unsticking level. These structures were induced by NW–dipping normal antithetic faults to the major SE–dipping normal Nîmes fault.

Due to the complex geology and the great depths, salt production there is often difficult. Cavern creep closure is very fast and leads to very high pressure within a few hours; typically, 200 bars (3000 psi) when the well is water-filled and when the wellheads are closed. Many strings were lost during operations, leading to fast upward displacement of cavern roof. A rise by hundreds of meters of cavern roof after a dozen of years is typical. Because lost string cannot be detected from the wellhead, logging operations are necessary at least once a year for each operating well to determine the final length of the well and the location of the cavern roof. Also, from time to time, non-halite plugs form in the casing, which sometimes leads to very costly workover operations.

From 1992 to 2011, permanent monitoring of seismic events has been managed by Magnitude company (Fortier et al., 2005), which allowed more than 60,000 events to be detected and located. This long monitoring period clearly demonstrated that local seismic activity at Vauvert is correlated with brine production (Figure 2).

Several preliminary testing campaigns performed by Brouard Consulting and Ecole Polytechnique showed that useable water hammers can be measured in these deep wells. Based on their results, it was decided, in 2011, to set up a permanent monitoring system on PA30-PA31 wells allowing early detection of any loss of string or plug development.

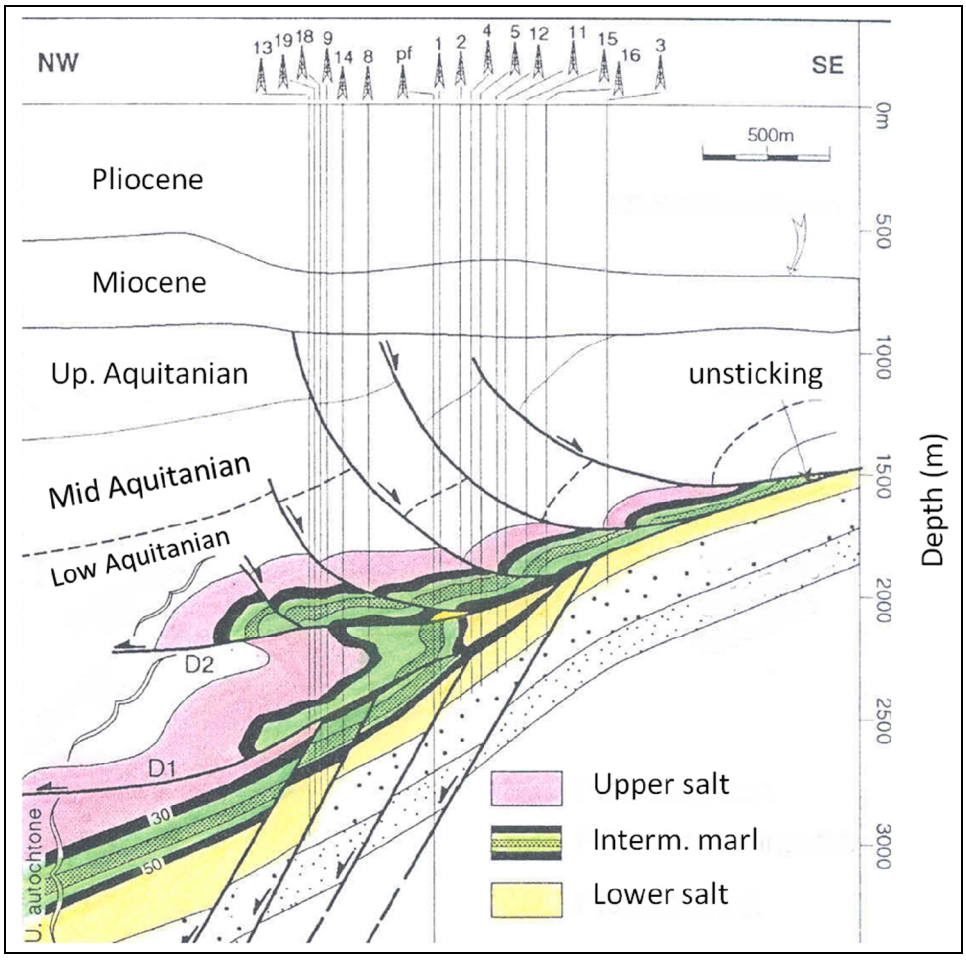

Figure 1. Geological section of the Vauvert field (after Valette, 1991).

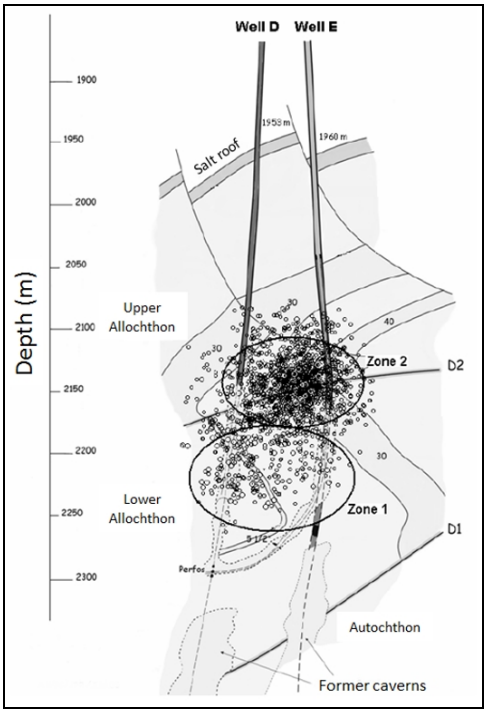

Figure 2. Example of seismic events recorded at Vauvert (after Fortier et al., 2005).

3.2 PA30-PA31 Wells

As most recent wells at Vauvert, PA30 and PA31 are deviated wells that start from the same platform (Figure 3 and Figure 4). An overview of well trajectories can be seen on Figure 5. PA30 is composed of two main sections (9-⅝" and 7") while PA31 has an additional final section (5").

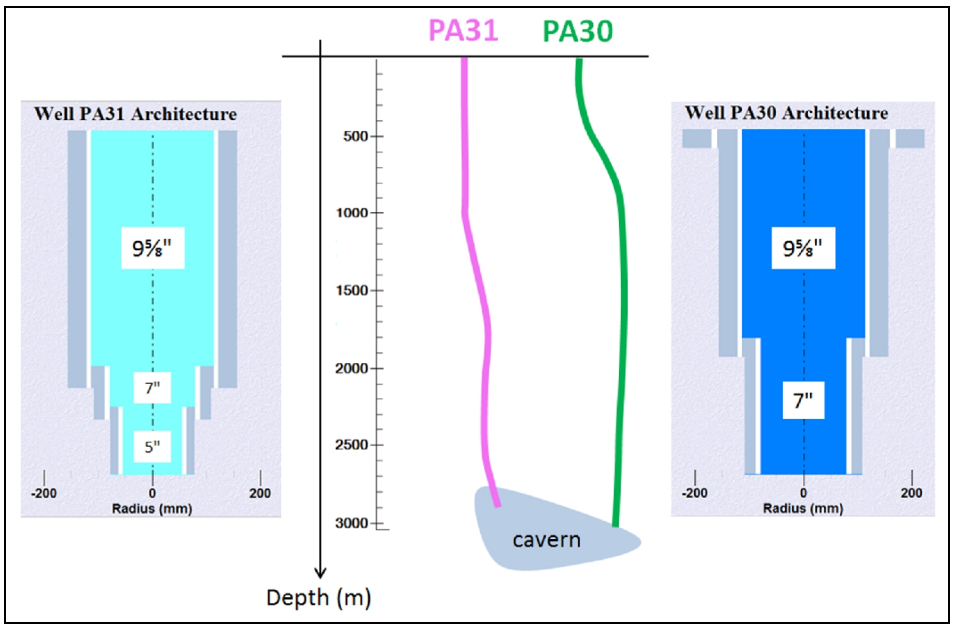

Figure 3. Schematic cross–section and completions of PA30–PA31 wells.

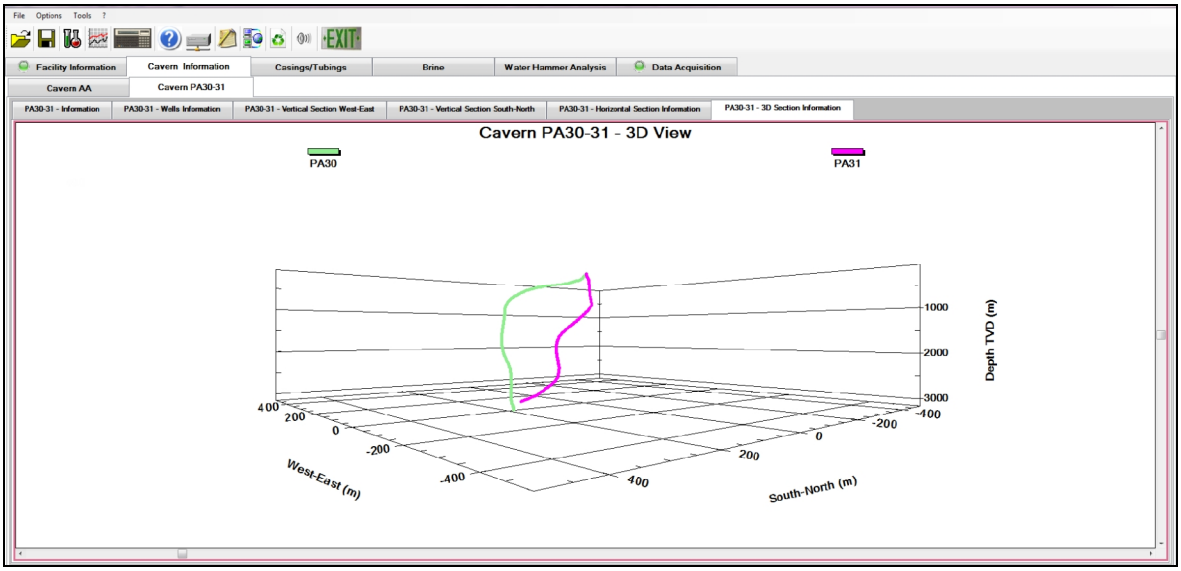

Figure 4. Screenshot – 3D view of PA30–PA31 wells.

3.3 Testing devices

The installed system consists of careful data collection at the two properly instrumented wells, filtering, spectral analysis to enhance and identify meaningful pressure oscillations in the data, and subsequent modeling to derive the final casing length and other possible information.

A dedicated quartz pressure gauge was set up on well PA31 to allow accurate recording of water hammers. A set of high-pressure valves also were plugged on this well. These serial valves are dedicated to the manual triggering of water hammers. The gauges are connected to the control room of the facility through buried cables (Figure 5). The dedicated data acquisition system in the control room records all data from the PA30-PA31 pairs — i.e., wellhead pressures (including the quartz gauge), temperatures and flow rates.

A dedicated computer also was installed in the head office and permanently connected to the acquisition system in the control room through a power-line Ethernet network. Furthermore, this computer was connected to Internet, allowing remote control from anywhere outside the facility. This allowed easy checking and updating of the system.

The system is able to detect and record any significant water hammer that would occur. A pre-trigger allows wellhead pressures to be recorded a few seconds before the detection of any event. Moreover, trigger sensitivity parameters can be set in the related page (Figure 6).

Signals are filtered, then the relevant ones are automatically analyzed and the final length of the well is computed.

Emails can also automatically be sent to a list of recipients when an important event is detected.

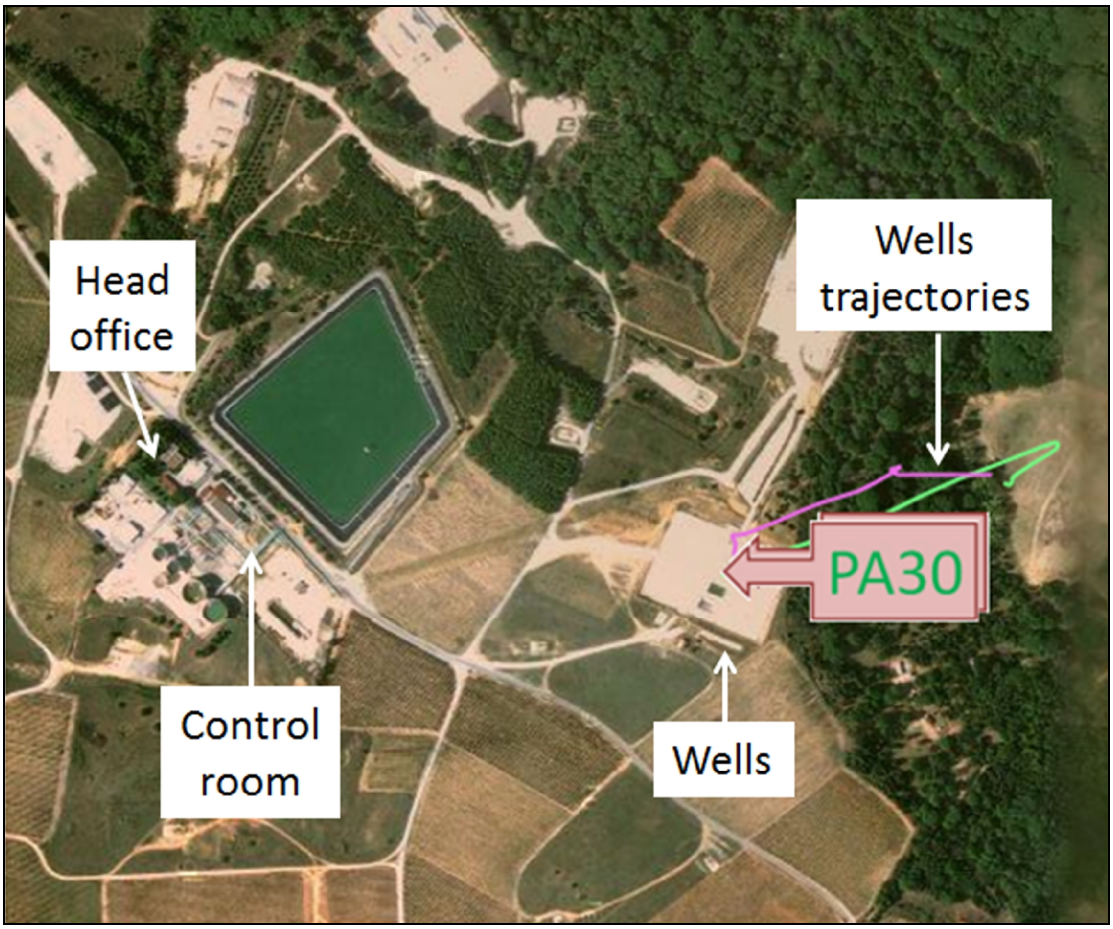

Figure 5. Overview of the Vauvert facility (Google Map).

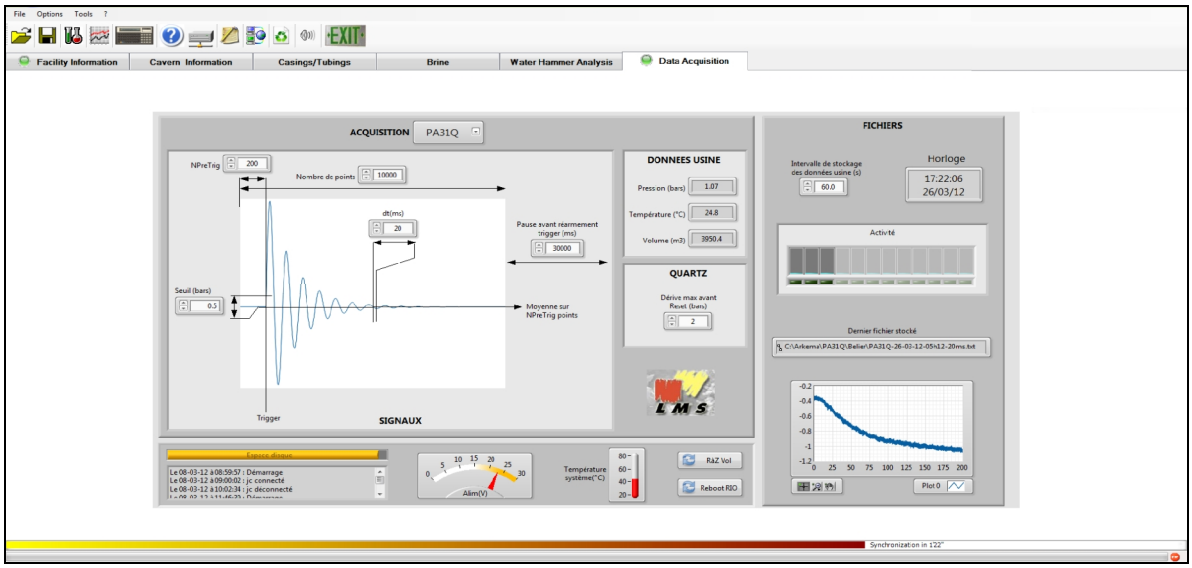

Figure 6. Screenshot of the software page dedicated to remote control of the data acquisition system.

3.4 Data acquisition and analysis software

The developed software allows the user to remotely control the acquisition system in the control room (Figure 6) to both display and analyze all acquired data. For each selected well, tables summarize all relevant recorded data and display the evolutions (Figure 7). With regard to water hammers, a power spectral analysis can be performed through standard FFT (Fast Fourier Transform) or Welch analysis (Figure 8). The period and power of the fundamental mode, T_1, and of the subsequent 3 harmonics, T_2 to T_4, are displayed in the table at the bottom right.

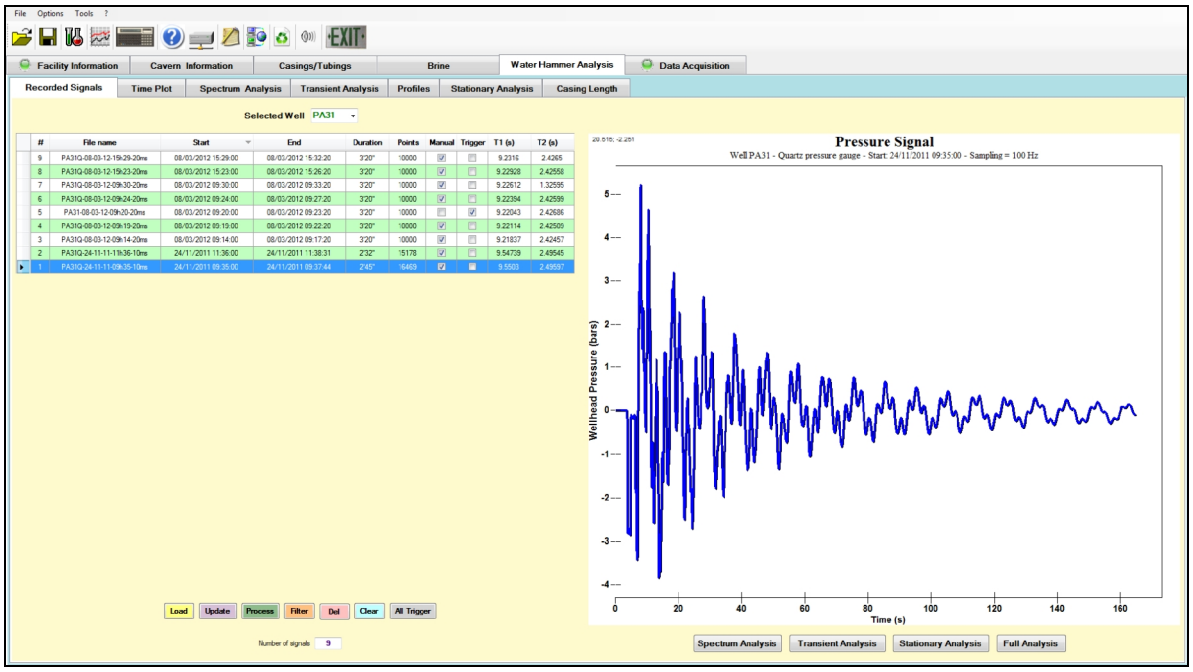

Figure 7. Screenshot of the PA31 water–hammer database.

3.5 Fluid properties as a function of depth

In order to link the spectral content of the pressure signals to the properties of the well, the vertical distributions of fluid properties must be considered. Because wells are very deep at Vauvert, liquid pressure can be very high, typically reaching more than 200 bars (3000 psi) at the wellhead and 450 bars (6500 psi) at a depth of 2500 m (8200 ft). The downhole temperature is also high, reaching above 120°C (250°F) at a 2500-m depth.

Calibration of the system is easier when the fluid in the well is at thermal equilibrium with the surrounding rock mass; it can be obtained when the well has been kept closed and idle for a few hours. Liquid temperature as a function of depth then is roughly equal to the natural vertical temperature distribution. The vertical distribution of the pressure subsequently can be calculated from the wellhead-measured value by progressive calculation of fluid density as a function of pressure and temperature. For a given pressure and temperature, the fluid adiabatic compressibility, β_f^{ad}, can be computed. The profile of the acoustic-wave celerity in the fluid (assuming no compressibility of the steel casing, or c_f) then can be calculated from equation (1). It is noticeable that for water and brine, this celerity is not a monotonic function of depth; for instance, it increases from 1430 m/s (4700 ft/s) to 1486 m/s (4900 ft/s) at a depth of approximately 600 m (2000 ft) and decreases to 1334 m/s (4375 ft/s) at a depth of 2500 m (8200 ft). Figure 10 shows a screenshot of these vertical distributions calculated for given wellhead data.

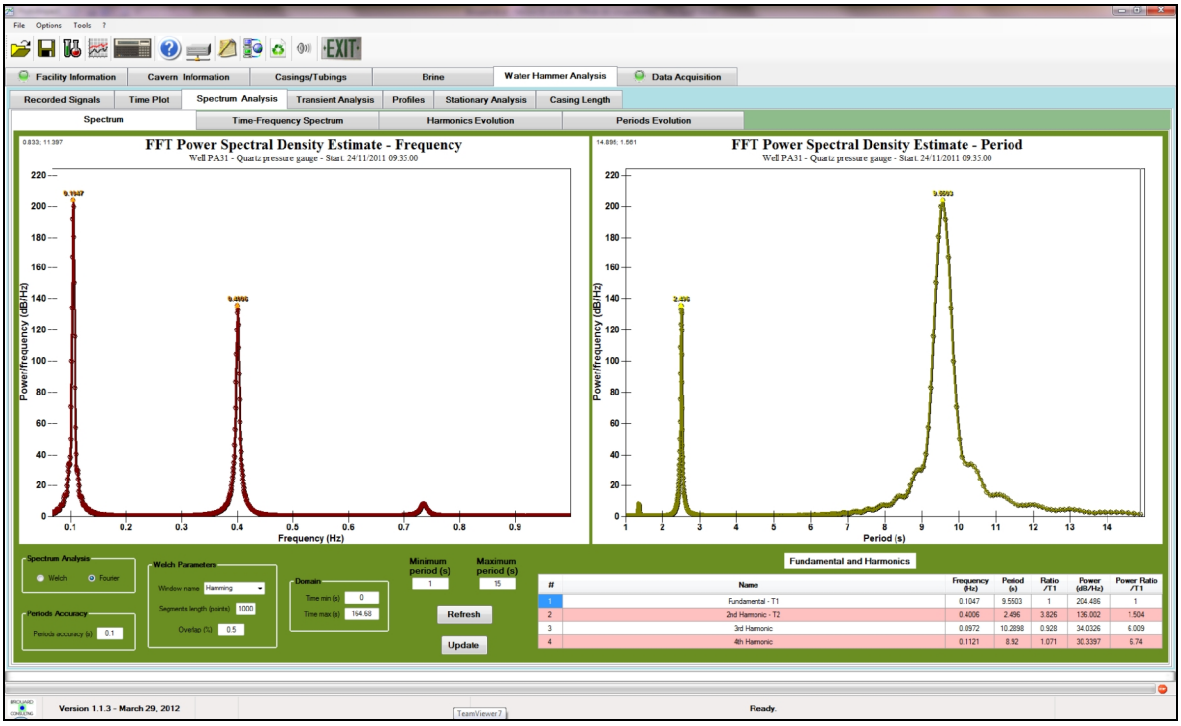

Figure 8. Screenshot of spectrum analysis: Power spectral density as functions of frequency (left) and period (right).

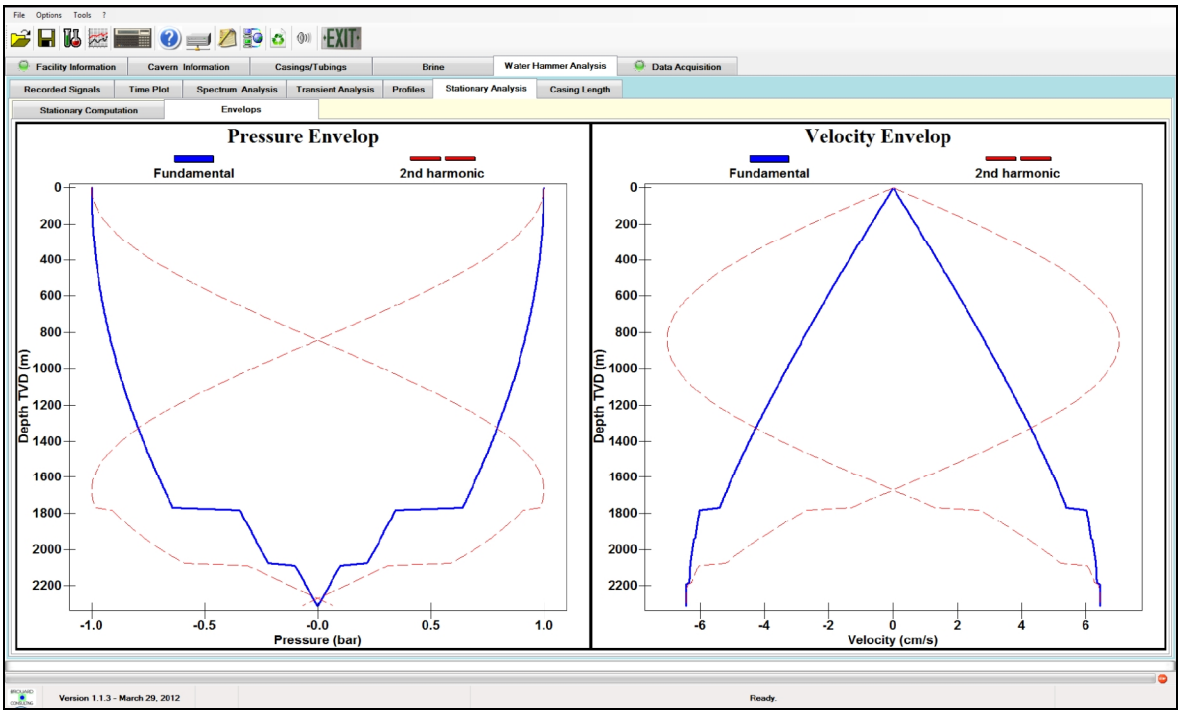

Figure 9. Screenshot: Stationary wave envelopes in the PA31 well.

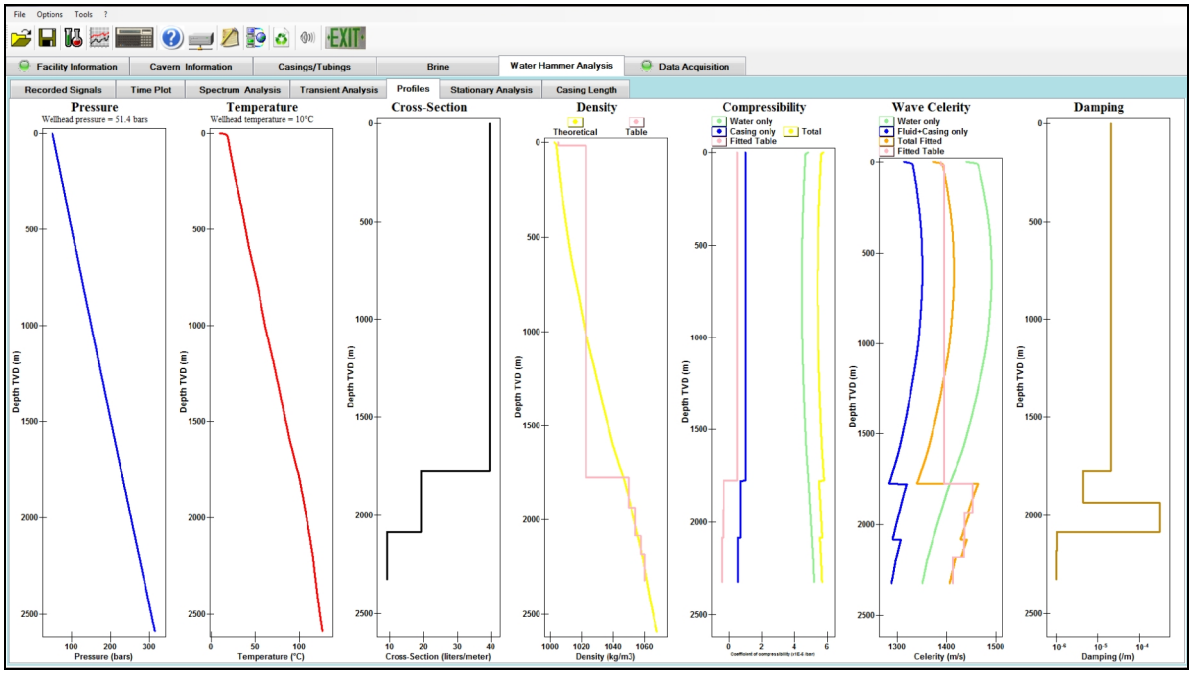

Figure 10. Screenshot – Computed vertical profiles. From left to right: fluid pressure, temperature, casing inner cross–section, fluid density, compressibilities, wave celerity, and damping.

3.6 Transient analysis

Very valuable information can be obtained from the analysis of the first seconds of a water hammer that has been triggered manually. An example is provided by Figure 11, in which the wellhead valve was left open for approximately 1.2 seconds. When it is assumed that well geometry experienced no change since leaching started, the computed pressure evolution is clearly late compared to the measured pressure evolution.

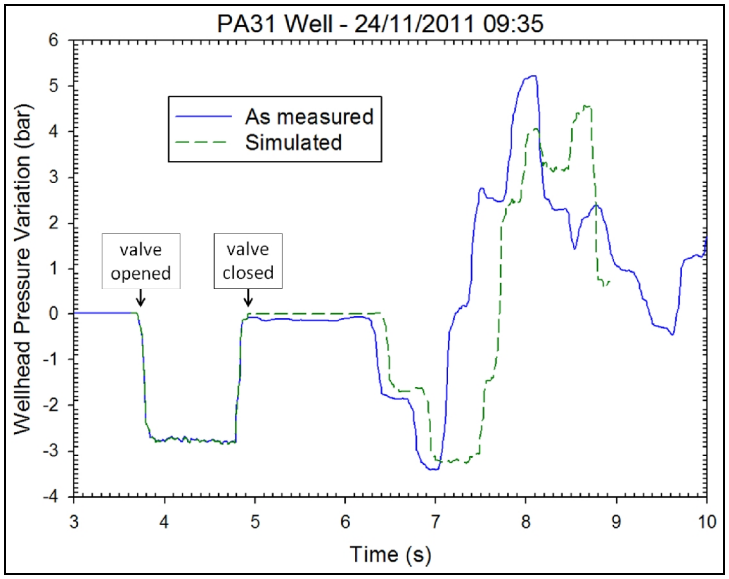

Figure 11. Comparison between measured and computed pressure evolutions. Well properties were estimated from initial well completion and assuming a well at thermal equilibrium.

Figure 12 shows wave celerities fitted using wave reflection at known depths — i.e., 1776.4 TVD depth (5828 ft) where the casing changes from 9-⅝" to 7" (Figure 4), and reflection at 2084.9 m TVD (6840 ft) where the casing changes from 7" to 5".

Figure 13 shows the final length of the well determined by extrapolating wave celeries from the overlying distribution and fitting the length of the last section. All these steps can be performed automatically by the software (Figure 14). In this example, it was back-calculated using the software that the final depth of the casing was 2352.9 m MD (2337.1 TVD). The logging operation performed by Schlumberger a couple of weeks later found the final length of the casing at 2352.8 m MD — i.e., **very close** to the computed figure.

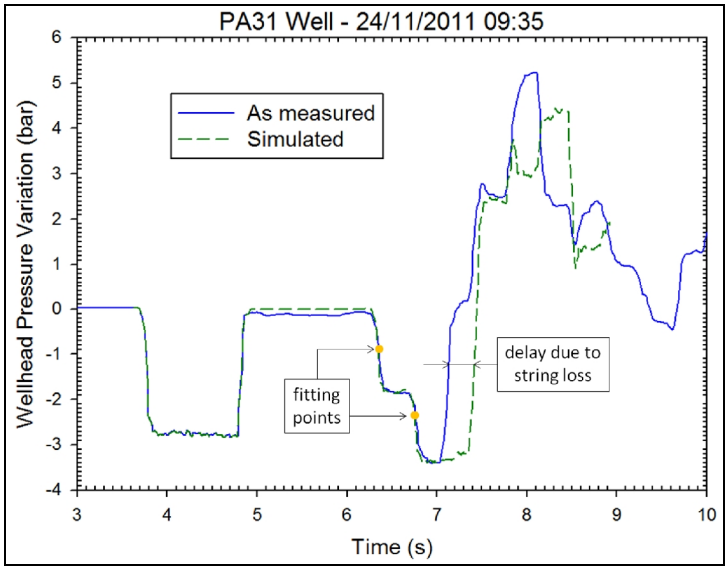

Figure 12. Comparison between measured and computed pressure evolutions after fitting the wave celerities in 9-⅝" and 7" sections. Onset of a delay after 7 s proves that strings were lost.

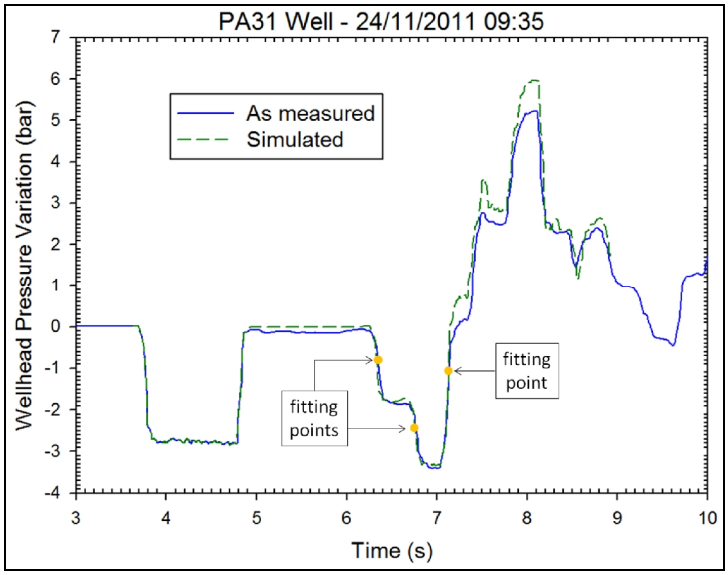

Figure 13. Comparison between measured and computed pressure evolutions after fitting the length of the last 5" section.

Figure 14. Screenshot of transient analysis: Comparison between measured and fitted pressure evolutions after damping back-calculation.

3.7 Stationary analysis

Stationary analysis of water hammers first calculates the theoretical frequencies in the pressure evolution signal. It is assumed that after a few seconds, the highest frequency components vanish, leaving a simpler wave whose periods are fixed by the boundary conditions.

A recurrence relation can be found from pressure continuity and flow conservation between each section. It allows for a given well geometry, especially a given final length, to determine the theoretical fundamental period, T_1, and the subsequent harmonic, T_2. Finally, the measured periods are used to determine the actual final length (Figure 15).

Stationary analysis can be especially helpful when the water hammer has not been triggered manually. This is the case, for instance, when a pump starts or stops. In that case, transient analysis cannot be performed; only stationary analysis can be used.

4. Other possible applications

The acquisition system and the software are designed for various types of configurations; examples are given in Figure 16.

In the case of a gas column, as a gas is less stiff that a liquid and dampening is higher, oscillations triggered by a water hammer are only a few seconds long. Thus, transient analysis is probably the most relevant. An asset of the method is that wave celerity in a gas column only depends on its temperature:

$$c_g = \sqrt{\gamma RT/\varpi} \tag{7}$$

where $\gamma = C_p/C_v$ is the ratio of heat capacities (typically, 1.4 for nitrogen or air and 1.27 for natural gas), R is the universal gas constant, T is absolute temperature of gas in Kelvins, and ϖ is the molar

mass of the gas. Additionally, because the heat capacity of a gas is significantly less than for a liquid, a gas column quickly comes to thermal equilibrium with the surrounding rock mass when it is kept idle.

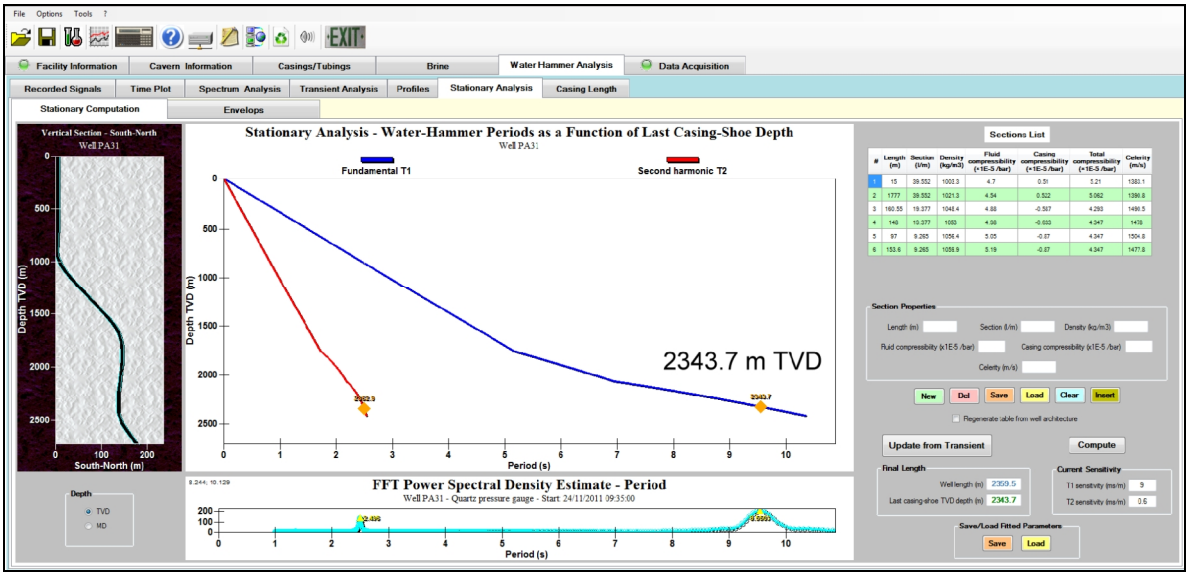

Figure 15. Screenshot of stationary analysis: Theoretical periods for fundamental mode and 2nd harmonic are computed as a function of final casing length compared to the spectrum of the measured signal.

5. Conclusions

Water hammers commonly are observed at wellheads. They often are considered as a potential hazard that should be avoided. Nevertheless, there are a few situations in which water hammers provide very valuable information about the well. A data acquisition system and a related user-friendly software code have been developed for the purpose of recording and analyzing water hammers. This device has been installed for the first time and successfully tested at the Vauvert brine field.

This paper demonstrates that this low-cost and non-intrusive system can be very accurate. Compared to other logging tools, it practically allows real-time measurement and can be controlled remotely.

Acknowledgements

The authors are indebted to the Arkema staff at the Vauvert brine field and to Jean-François Beraud, whose help in setting up the system was invaluable.

References

Bérest P., Bergues J. and Brouard B. (1996) *Vibrations and free oscillations in salt caverns*. SMRI Fall Meeting, SMRI, Cleveland, OH, 311–335.

Bérest P., Bergues J. and Brouard B. (1999) *Static and dynamic compressibility of deep underground caverns*. International Journal of Rock Mechanics and Mining Sciences, Elsevier, Vol. 36, 1031–1049.

Fortier E., Maisons C. and Valette M. (2005) *Contribution to a better understanding of brine production using a long period of microseismic monitoring*. Proc. SMRI Fall Meeting, Nancy, France.

Ghidaoui, M.S., *Zhao Ming*, McInnis, D.A, and *Axworthy, H.H.* (2005). *A Review of Waterhammer Theory and Practice. Applied Mechanics Review*, Transactions of the American Society of Mechanical Engineers (ASME), 58, 49–76.

Joukowski N. E. (1898) *Memoirs of the Imperial Academy Society of St. Petersburg*. Russian translated by O. Simin 1904. Proc. Amer. Water Works Assoc. 24, 341–424.

Ratigan J.L. (2008). Brine String Integrity and Model Evaluation. Proc. SMRI Fall Meeting, Galveston, TX, 273-293.

Tait R. J., Bryant Moodie T. and Haddow J. B. *Wave* (1981) *Propagation in a Fluid–Filled Elastic Tube*. Acta Mechanica Vol. 38, Numbers 1–2, DOI: 10.1007/BF01351463, Springer Wien, 71–83.

Valette M. (1991) *Etude structurale du gisement de Vauvert* (in French). PhD Thesis, Montpellier II University.

Van Sambeek L., Bérest P. and Brouard B. (2005) *Improvements in Mechanical Integrity Tests for Solution–Mined Caverns Used for Mineral Production or Liquid–Product Storage.* Report for The Solution Mining Research Institute, Topical Report RSI–1799, 142 pages.

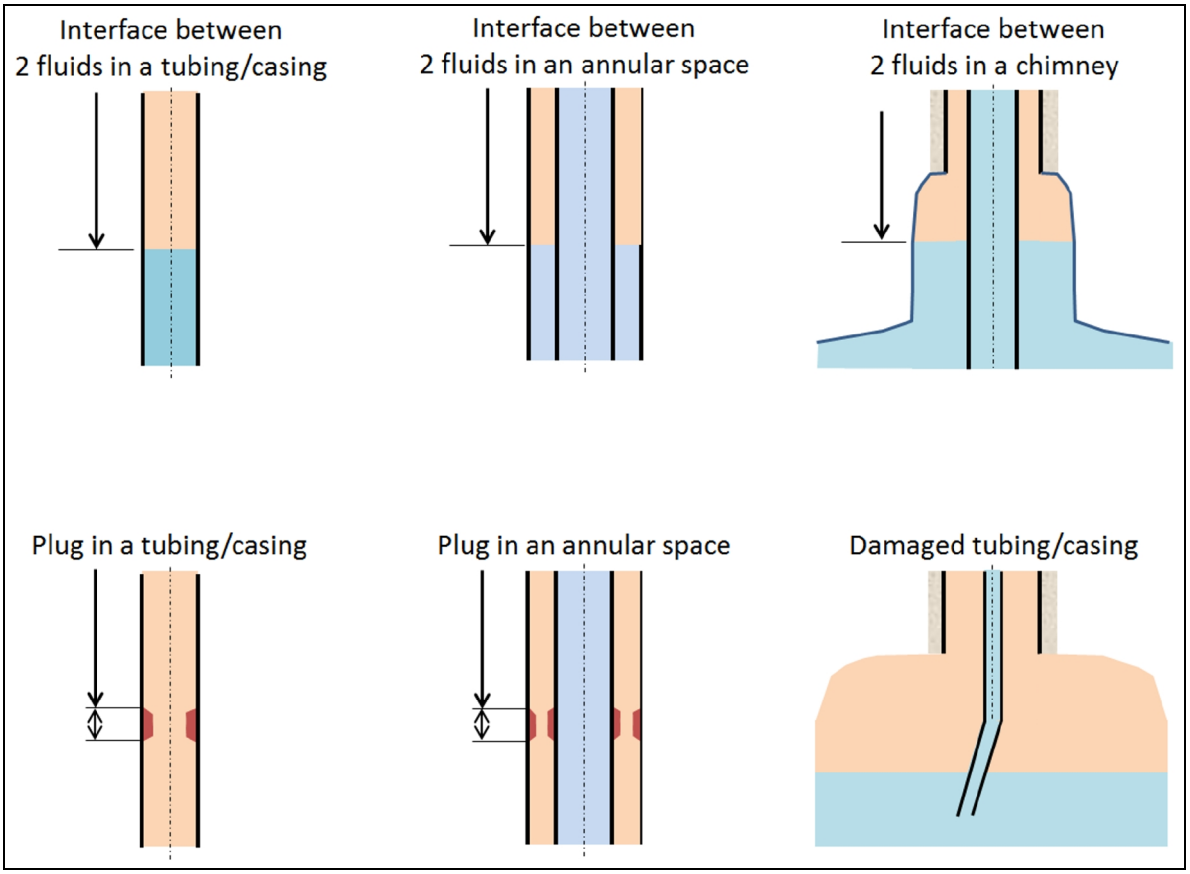

Figure 16. Examples of configuration where water-hammer analysis can be helpful.